JOURNAL OF AGRICULTURAL AND FOOD CHEMISTRY

Article

pubs.acs.org/JAFC

Preparation of Microfibrillated Cellulose/Chitosan−Benzalkonium Chloride Biocomposite for Enhancing Antibacterium and Strength of Sodium Alginate Films

Kai Liu, Xinxing Lin, Lihui Chen, Liulian Huang,* Shilin Cao, and Huangwei Wang

College of Materials Engineering, Fujian Agriculture and Forestry University, Fuzhou 350002, China

ABSTRACT: The nonantibacterial and low strength properties of sodium alginate films negatively impact their application for food packaging. In order to improve these properties, a novel chitosan−benzalkonium chloride (C−BC) complex was prepared by ionic gelation using tripolyphosphate (TPP) as a coagulant, and a biocomposite obtained through the adsorption of C−BC complex on microfibrillated cellulose, MFC/C−BC, was then incorporated into a sodium alginate film. The TEM image showed that the C−BC nanoparticles were spherical in shape with a diameter of about 30 nm, and the adsorption equilibrium time of these nanoparticles on the surface of MFC was estimated to be 6 min under the driving forces of hydrogen bonds and electrostatic interactions. According to the disc diffusion method, the MFC/C−BC biocomposite-incorporated sodium alginate film exhibited remarkable antibacterial activity against *Staphylococcus aureus* and certain antibacterial activity against *Escherichia coli*. The strength tests indicated that the tensile strength of the composite sodium alginate film increased about 225% when the loading of MFC/C−BC biocomposite was 10 wt %. These results suggested that the MFC/C−BC biocomposite-incorporated sodium alginate film with excellent antibacterial and strength properties would be a promising material for food packaging, and the MFC/C−BC may also be a potential multifunctional biocomposite for other biodegradable materials.

KEYWORDS: *microfibrillated cellulose, chitosan, sodium alginate, antibacterial activity, tensile strength*

INTRODUCTION

Solid packaging waste has become a global environmental problem due to its nonbiodegradability.[1−3] Much effort has made to develop biodegradable materials such as sodium alginate, starch,[4,5] agar,[6,7] and hemicellulose.[8] Sodium alginate is water-soluble, nontoxic, biocompatible, and reproducible and can be used to produce a film for food packaging because of its unique colloidal and excellent membrane-forming properties.[9,10] However, its strength property is naturally limited and it has no inherent antibacterial properties.[11] Some researchers have attempted to improve these shortcomings of sodium alginate films. For example, Fayaz[12] studied the synthesis of silver nanoparticles and their incorporation into sodium alginate films for vegetable and fruit preservation. They found that the silver nanoparticles incorporated within the sodium alginate thin film showed promising antibacterial activity against test strains. Wang[13] prepared the composite biodegradable films using whey protein isolate, gelatin, and sodium alginate and assessed the strength property of these composite films. Most studies have focused solely on developing films with a single function, such as strength or antibacterial property. Thus, it would be greatly beneficial to look forward to developing more multifunctional biodegradable films for a wider variety of applications.

Microfibrillated cellulose (MFC) is a new form of expanded high-volume cellulose, moderately degraded and greatly expanded in surface area, obtained through a homogenization process.[14,15] Previous research has demonstrated that MFC can be used as a reinforcing medium in composites because it consists of aggregates of cellulose microfibrils with a diameter of 20−60 nm and has a very good ability to form a weblike network.[16,17] In addition, MFC can easily adsorb positively charged polymers, such as chitosan, by hydrogen bonds and electrostatic interactions between the MFC and the chitosan.

Chitosan (C) is the second most abundant natural biopolymer after cellulose and is also an edible and biodegradable material that has antimicrobial properties against bacteria and molds.[18−20] Besides the commonly used synthetic polymers, chitosan has been largely favored as a particle carrier because of its good biocompatibility and hydrophilic property.[21−23] In recent years, research has predominantly focused on the production of nanoparticles using chitosan for the delivery of proteins, peptides, and plasmids.[24−26]

In an attempt to enhance the antimicrobial property while the high strength of the sodium alginate film is maintained, chitosan was ionically cross-linked with tripolyphosphate (TPP) for the encapsulation of benzalkonium chloride, since benzalkonium chloride is highly water soluble and active against bacteria and some viruses, fungi, and protozoa.[27] The chitosan−benzalkonium chloride (C−BC) complex was then adsorbed on the MFC surface through electrostatic interactions and hydrogen bonds, and the multifunctional sodium alginate films were produced by incorporating the MFC/C−BC biocomposite into the sodium alginate. The aim of the present study was to prepare a novel MFC/C−BC biocomposite and investigate the antibacterial and strength properties of sodium alginate-based food packaging films containing MFC/C−BC biocomposite.

Received: March 5, 2013
Revised: June 10, 2013
Accepted: June 10, 2013
Published: June 10, 2013

dx.doi.org/10.1021/jf4010065 | *J. Agric. Food Chem.* 2013, 61, 6562−6567

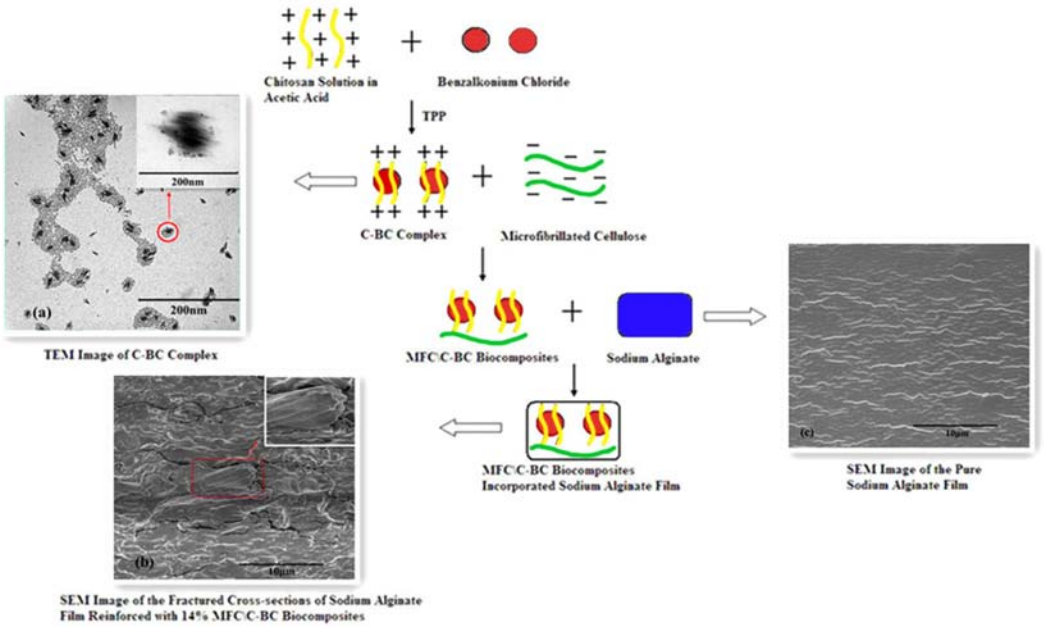

Figure 1. Preparation scheme of MFC/C−BC biocomposite-incorporated sodium alginate film.

MATERIALS AND METHODS

Materials. Chitosan (MW = 7×10^5 Da, degree of deacetylation = 95%) was purchased from Yuhuan Ocean Biochemical Co., Ltd. Sodium alginate (SA) and benzalkonium chloride (BC) were provided by Aladdin reagent Co., Ltd. Microfibrillated cellulose (MFC, Celish KY100G, 10 wt % solid slurry) was gifted by Daicel Chemical Industries, Ltd. All other chemicals were of analytical grade and used without further purification.

Methods. *Preparation of Chitosan−Benzalkonium Chloride (C−BC) Complex.* Chitosan solution was prepared by dissolving 0.4 g of chitosan flakes in 100 mL of 1% (v/v) acetic acid at 30 °C. Then 10 mL of 40 g/L (w/v) benzalkonium chloride solution was added and stirred at a stirring rate of 150 rpm. After 0.5 h, 40 mL of 2 g/L tripolyphosphate solution was added into the above solution and stirred for 4 h to obtained 150 mL of C−BC complex solution.

Characterization of C−BC Complex. For transmission electron microscopy (TEM), the sample was prepared by placing a drop of colloidal solution of C−BC complex on a copper grid and allowing it to completely dry at room temperature. The image of the sample was obtained using a transmission electron microscope (JEOL JEM-1010), operating at 80 kV. The FTIR spectra of chitosan, benzalkonium chloride, and C−BC complex were recorded using Fourier transform infrared spectroscopy (Thermo Nicolet 360) at a resolution of 4 cm^{-1} in the spectral region of 500−4000 cm^{-1}, by making a KBr pellet of each sample. Thermogravimetric analysis (TGA) of chitosan, benzalkonium chloride, and C−BC complex was performed on a TG−DTA Instruments (Netzsch STA 449F3). Approximately 5 mg of sample was weighed and heated from room temperature to 700 °C at a heating rate of 10 °C/min under a nitrogen flow rate of 20 mL/min.

Surface Charge Density Measurement. The ζ-potentials of the resulting C−BC complex in solution and MFC were measured using a Zetasizer Nano-ZS (Malvern). The charge density was measured as follows. One milliliter of C−BC solution or MFC (1 wt %) was extracted with a pipet, diluted 10-fold with distilled H_2O, and titrated with 0.001 N poly(diallyldimethylammonium chloride) (poly-DADMAC) or potassium polyvinyl sulfate (PVSK) by using a Mütek particle charge detector (PCD-04) and titrator (PCD-T).

Preparation of MFC/Chitosan−Benzalkonium Chloride (MFC/C−BC) Biocomposite. The 10 wt % MFC was diluted 10-fold with distilled H_2O to obtain 1 wt % solid slurry. Then 50 g of 1 wt % MFC suspension was added into 150 mL of C−BC complex solution. The resulting suspension was subsequently incubated at room temperature and kept stirring at a rate of 150 rpm for 1 h. At the end of incubation, the MFC/C−BC biocomposite was separated by centrifuging at 4000 rpm for 10 min. The content of nitrogen in supernatant C−BC complex was determined by the Kjeldahl method. The content of nitrogen was calculated by the formula[28]

$$\mathrm{N\%} = \frac{VC \times 14.007 \times 10^{-3} \times 100}{W}$$

where V is the volume of hydrochloric acid solution (HCl) used in titration for C−BC complex (mL), C is the concentration of standard HCl solution (mol/L), and W is the weight of testing sample (g).

Preparation of MFC/C−BC Biocomposite-Incorporated Sodium Alginate Film. One gram of sodium alginate (SA) powder was solubilized in 49 mL of distilled water to obtained 2 wt % solution of SA, and 0.5 g of glycerol was then added into the SA solution at a glycerol:SA powder ratio of 1:2 (w:w). The solution was stirred continuously and heated to 80 °C for 0.5 h using a magnetic stirrer hot plate, until the SA powder was completely dissolved. The MFC/C−BC biocomposite suspension (0.5 wt %) was added to the SA solution and stirred mechanically (PT3100D, Kinematica AG) and then dispersed by ultrasonic treatment (KQ-250DB, Kun Shan Ultrasonic Instruments Co., Ltd., 40 kHz) for about 5 min with 100% power level. The films were cast on a round glass plate with a diameter of 15 cm by the hand casting method from the mixture of the MFC/C−BC biocomposite and SA solution. After keeping the films at room temperature for 12 h, the films were kept in a dry-oven at 50 °C for 12 h. Prior to strength testing, the films were conditioned at 50% relative humidity and 25 °C. The composites with four levels of MFC/C−BC biocomposite loading (2%, 6%, 10%, and 14% based on SA powder weight) were prepared. Film thickness was measured using a micrometer with 0.001 mm resolution.

Antibacterial Property of the MFC/C−BC Biocomposite-Incorporated Sodium Alginate Film. To examine the antibacterial effect of the composite films, *Escherichia coli* ATCC 8739 and *Staphylococcus aureus* ATCC 6538, Gram-negative and Gram-positive organisms, respectively, were used as the test organisms. Nutrient agar medium was prepared by dissolving 14 g of agar, 3 g of beef broth, 10 g of peptone, and 5 g of NaCl in 1 L of distilled water. The pH of the solution was then adjusted to 7.0. The agar medium was transferred into Petri plates in quantities of 15 mL and left on a flat surface to completely solidify. The bacteria were grown in broth for 24 h at 37 °C and further diluted to get a concentration of about 10^5 cfu/mL with NaCl solution (0.85%, w/v). They were then transferred and spread onto the solid surface of the agar medium. A disc (8.5 mm diameter)

dx.doi.org/10.1021/jf4010065 | J. Agric. Food Chem. 2013, 61, 6562−6567

was punched out of a MFC/C−BC biocomposite-incorporated sodium alginate film or pure sodium alginate film and was centrally placed on the solid agar plates, previously seeded with individual test bacteria. After incubation at 37 °C for 24 h, the zones of inhibition were observed.

SEM Analysis. The morphology of the fractured surfaces of the MFC/C−BC biocomposite-incorporated sodium alginate film and pure sodium alginate film was investigated using a scanning electron micrograph (Nova NanoSEM 230, FEI). The films were cryofractured in liquid nitrogen. The fractured surfaces were then coated with gold on an ion sputter coater, and operating voltages of SEM were 5 kV. Magnification of 10 000× was used.

Tensile Properties. The tensile properties of the MFC/C−BC biocomposite-incorporated sodium alginate films and pure sodium alginate films were measured using a strength testing machine (DCP-KZ 300, Sichuan Changjiang Paper Instrument Co., Ltd.). Tensile deformation was determined at a crosshead speed of 10 mm/min. The samples were cut to shape with a width of 15 mm and length of 150 mm. Five composite specimens were tested. For each composition, at least five replicates were tested, and the results are presented as the average of the tested samples.

RESULTS AND DISCUSSION

Preparation of MFC/C−BC Biocomposite-Incorporated Sodium Alginate Film. An illustrative scheme of MFC/C−BC biocomposite-incorporated sodium alginate film is shown in Figure 1. The C−BC complex was prepared by an ionic gelation method using tripolyphosphate (TPP), and the TEM image of C−BC complex is shown in Figure 1a. It was found that C−BC nanoparticles were spherical in shape with a diameter of about 30 nm. Then, the MFC was used to adsorb the C−BC complex to obtain the MFC/C−BC biocomposite. Hydrogen bonds and electrostatic interactions between the MFC and the C−BC complex may be the driving forces for the adsorption.[29] Finally, the MFC/C−BC biocomposite was incorporated into sodium alginate film to enhance the antibacterial and strength properties of the film.

Parts b and c of Figure 1 show the SEM images of the cross-section image of fracture surfaces of MFC/C−BC biocomposite-incorporated sodium alginate film and pure sodium alginate film, respectively. As compared to the pure sodium alginate film (Figure 1c), the morphology of the MFC in the sodium alginate matrix can be easily identified; the MFC was dispersed uniformly in the sodium alginate film, and there were no gaps between the sodium alginate matrix and MFC (Figure 1b). Cheng[30] studied the effect of cellulose fibrils in micro- and nanoscale reinforcement of latex of poly(vinyl alcohol) (PVA) and found that the presence of a gap between cellulose fibrils and polymers enabled noneffective reinforcement of the matrix and achieved a decrease of the tensile strength of PVA. Thus, as can be speculated on the basis of the SEM images (Figure 1b), the MFC/C−BC biocomposite not only enabled effective reinforcement but also provided a remarkable antibacterial activity for the sodium alginate film.

FTIR Analysis of the C−BC Complex. The complex of chitosan and benzalkonium chloride was first investigated using FTIR spectroscopy. As seen in Figure 2, for the IR spectrum of chitosan, characteristic peaks were found at 1650, 1601, and 1380 cm^{-1} correspond to amide I, II, and III, respectively.[25] Two other characteristic peaks of chitosan appear at 3387 cm^{-1} (O−H stretch overlapped with N−H stretch) and 2876 cm^{-1} (C−H stretch).[27] In the spectrum of benzalkonium chloride, the characteristic peaks appear at 1458 cm^{-1} (C═C stretch), 1000 cm^{-1}(C−N stretch), and 2925 cm^{-1} (−CH_3 bend). After the complex was formed, the major changes in the FTIR

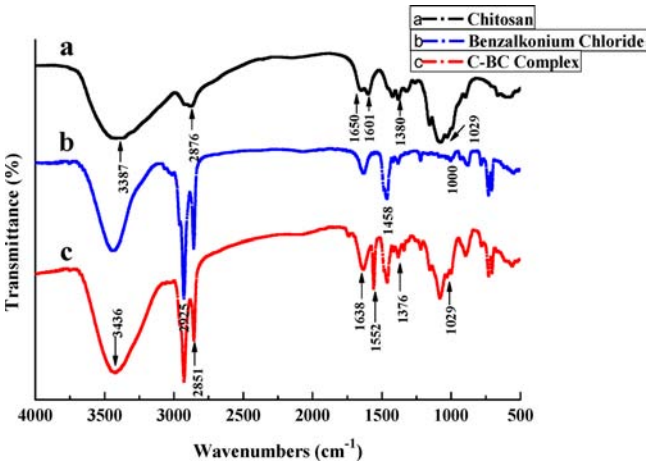

Figure 2. FTIR spectra of (a) chitosan, (b) benzalkonium chloride, and (c) C−BC complex.

spectra for the complex were that the characteristic peaks of chitosan at 1650 cm^{-1} (amide I), 1601 cm^{-1} (amide II), and 1380 cm^{-1} (amide III) were shifted to 1638, 1552, and 1376 cm^{-1}, respectively, and the characteristic peaks of chitosan at 3387 and 2876 cm^{-1} were also shifted to lower wavenumber (3436 and 2851 cm^{-1}). Furthermore, the intensity of the −C−OH stretching (1029 cm^{-1}) band on the chitosan chain became weaker. The changes that occurred at the hydroxyl (−C−OH) and amino groups of chitosan were probably influenced by the presence of −P−OH groups from TPP. These results indicated that benzalkonium chloride was immobilized into chitosan by ionic gelation using tripolyphosphate (TPP) and was entrapped in gel. These kinds of chitosan nanoparticles encapsulated by benzalkonium chloride were successfully prepared by electrostatic complexation of tripolyphosphate and chitosan for the first time, as oppositely charged polyelectrolytes can form stable intermolecular complexes.[25,27]

Thermal Stability of C−BC Complex. Thermogravimetric (TG) and derivative thermogravimetric (DTG) curves of chitosan, benzalkonium chloride, and C−BC complex are shown in Figure 3. The results indicated 4, 36, and 16 wt % degradation of chitosan and 7, 84, and 5 wt % degradation of benzalkonium chloride during the first, second, and third step, respectively. The degradation of chitosan and benzalkonium chloride took place at 295 and 208 °C, respectively. However, 11, 41, and 12 wt % degradation of C−BC complex was observed during the first, second, and third step, respectively, and the degradation of C−BC complex took place at 197 °C. The chitosan and C−BC complex showed slow weight loss starting from room temperature to about 150 °C in the first step, mainly due to water loss.[31] It was noted that the lower degradation temperature and larger weight loss in second step for benzalkonium chloride showed its poor thermal stability compared with chitosan. Thus, with the complex of chitosan and benzalkonium chloride, the process of weight loss (41 wt %) for C−BC complex during the second step was faster than that of chitosan (36 wt %), and the weight loss (84 wt %) for benzalkonium chloride during second step was greater than that of C−BC complex (41 wt %). Furthermore, the chitosan and C−BC complex showed obvious loss of weight during the second step, which could be attributed to decomposition of benzalkonium chloride and acetylated and deacetylated units of chitosan. Sun[31] studied the thermal stability of chitosan−guanidine complexes and found the similar results.

dx.doi.org/10.1021/jf4010065 | J. Agric. Food Chem. 2013, 61, 6562−6567

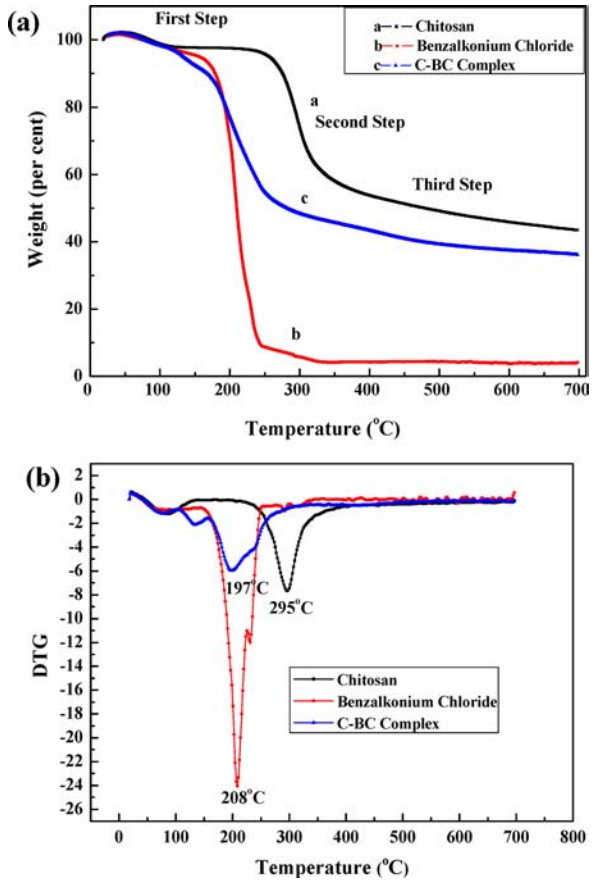

Figure 3. TG (a) and DTG (b) spectra of chitosan, benzalkonium chloride, and C−BC complex.

Kinetics of Adsorption of C−BC Complex on MFC. The preparation of MFC/C−BC biocomposite is based on the adsorption of polyelectrolytes of opposite charge. Thus, it is very important to determine the surface charge density of both polyelectrolytes for the adsorption in polyelectrolyte systems. Potentiometric titration and ζ-potential, the common methods to measure the surface charge density of polyelectrolytes,[29] were used to characterize quantitatively the surface charge density of both C−BC complex and MFC. For C−BC complex, the charge density and ζ-potential were 1.6 mequiv L^{-1} and +21.3 mV, respectively. However, the charge density and ζ-potential value of MFC were found to be 0.3 mequiv L^{-1} and −17.4 mV, respectively, which were different from the values reported in other literature;[29] this was mainly due to the different production methods of the nanofibers. Therefore, the charge density and ζ-potential of C−BC complex were greater than those of the MFC because of the large amounts of $-NH_3^+$ functional groups present in chitosan with a high degree of deacetylation (95%), and the C−BC complex with high positive charge was easily adsorbed on the surface of the MFC with negative charge through electrostatic interactions and hydrogen bonds.

It was very important to estimate the adsorption equilibrium time of C−BC complex on the MFC surface for the preparation of MFC/C−BC biocomposite. This estimation was based on the Kjeldahl method, which was used to determine the nitrogen content of C−BC complex in the supernatant. Figure 4 shows the adsorption kinetics of C−BC complex on the MFC surface; it was found that the nitrogen content in supernatant decreased

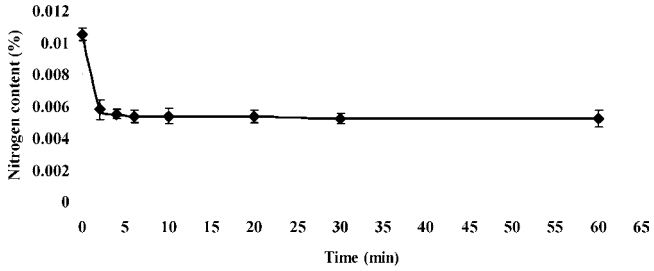

Figure 4. Adsorption kinetics of C−BC complex on MFC.

rapidly with the increase of the absorption time, and this was mainly due to the reduction of the C−BC complex in supernatant after the adsorption of the C−BC complex on the MFC. The nitrogen content of C−BC complex in supernatant did not decrease any more after 6 min, and thus the adsorption equilibrium time was estimated to be 6 min. A similar equilibrium time for chitosan adsorbed on CNWs films also can be found in the literature.[29] However, 20 min was chosen for the preparation time of MFC/C−BC biocomposite in order to ensure the adsorption equilibrium.

Tensile Properties of MFC/C−BC Biocomposite-Incorporated Sodium Alginate Film. The tensile strength values of sodium alginate and its composites reinforced by MFC/C−BC biocomposite of 2, 6, 10, and 14 wt % are shown in Figure 5. The tensile strength of sodium alginate film was

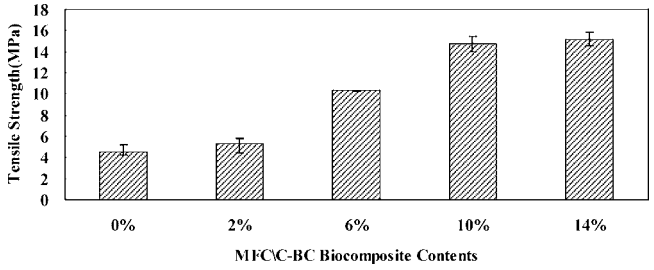

Figure 5. Tensile strength of pure sodium alginate film and MFC/C−BC biocomposite-reinforced sodium alginate films at 2, 6, 10, and 14 wt % loading.

4.53 MPa and it was increased significantly by the weight contents of MFC/C−BC biocomposite. The tensile strength of MFC/C−BC biocomposite-reinforced sodium alginate films reached the highest value (14.72 MPa) at the loading of 10 wt %, and this value was about 225% higher than that of sodium alginate film. When the loading of the biocomposite to sodium alginate matrix achieved 14%, the tensile strength did not increase any more. The results indicated that the MFC would be an excellent material for enhancing the strength property of sodium alginate film.

It should be emphasized that the MFC/C−BC biocomposite loading of 2 wt % to sodium alginate matrix slightly increased the tensile strength of the sodium alginate film. However, when the loading of the biocomposite reached 6 wt %, the tensile strengths of sodium alginate film was 127% higher compared to the pure sodium alginate film. Iwatake[32] studied the typical morphology of the MFC and found that MFC completely disintegrated into nano- to submicrometer wide fibers and could create a fine network. Samir[33] pointed out that cellulose nanofiber can be used as a reinforcement due to the additional entanglement effect of the elements. Therefore, the additional entanglement effect induced by MFC with a weblike network

dx.doi.org/10.1021/jf4010065 | J. Agric. Food Chem. 2013, 61, 6562−6567

may be not enough for reinforcement of the sodium alginate film, as the loading of MFC/C−BC biocomposite was only 2 wt %. However, when the MFC/C−BC biocomposite content achieved 6 wt %, the reinforcement effect on the sodium alginate film was pronounced.

Antibacterial Activity of MFC/C−BC Biocomposite-Incorporated Sodium Alginate Film. The antibacterial activities of MFC/C−BC biocomposite-incorporated sodium alginate films and pure sodium alginate films against *E. coli* and *S. aureus* were tested by the disc diffusion method,[34,35] as seen in Figure 6. It was found that there was no inhibition zone

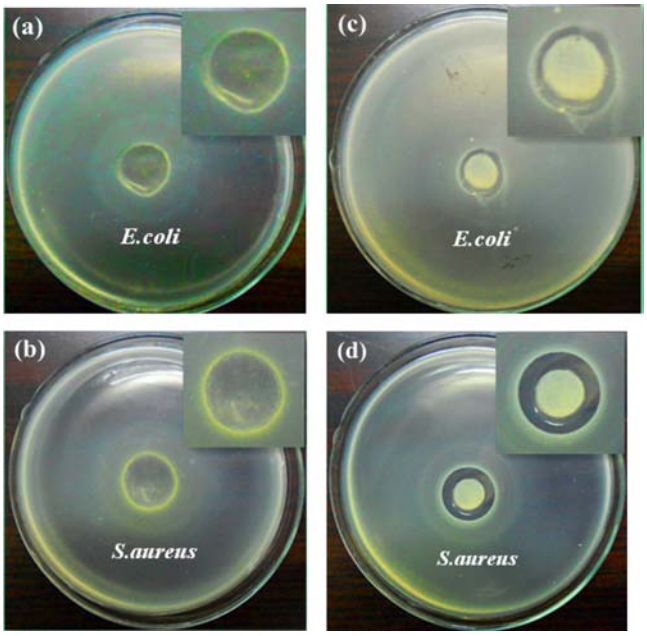

Figure 6. The antibacterial activities of pure sodium alginate film against *E. coli* (a) and *S. aureus* (b) and of MFC/C−BC biocomposite-incorporated sodium alginate film at 10 wt % loading against *E. coli* (c) and *S. aureus* (d).

around the pure sodium alginate film (Figure 6a,b), whereas two inhibition zones can be observed around the MFC/C−BC biocomposite-incorporated sodium alginate film (Figure 6c,d). However, there was some difference in the inhibition activity against *E. coli* and *S. aureus* for the sodium alginate composite film. The diameter of inhibition against *S. aureus* (Figure 6d) was significantly larger than that against *E. coli* (Figure 6c). This was mainly due to Gram-positive bacteria generally being more susceptible to benzalkonium chloride than Gram-negative bacteria. As a result, the MFC/C−BC biocomposite-incorporated sodium alginate film exhibited a remarkable antibacterial activity against *S. aureus* and certain antibacterial activity against *E. coli*, respectively.

It was reported that chitosan was an edible and biodegradable material that had antimicrobial activity against bacteria and molds, and the antibacterial mechanism was suggested to be an electrostatic interaction between $-NH_3^+$ groups of chitosan and phosphoryl groups of phospholipid components of cell membranes; however, chitosan would show high antibacterial activity only under acidic condition.[36] In addition, benzalkonium chloride was also an antibacterial agent and has been extensively used in antimicrobial materials.[37] The mechanism of its bactericidal effect is thought to be disruption of intermolecular interactions. This disruption can cause dissociation of cellular membrane bilayers.[38] In this study, the complex of chitosan and benzalkonium chloride was obtained by ionic gelation. After being adsorbed on the MFC and added into the sodium alginate, benzalkonium chloride could further enhance the antibacterial activity of the sodium alginate film.

In conclusion, a novel multifunctional MFC/C−BC biocomposite was successfully prepared and can be dispersed uniformly in the sodium alginate through mechanical stirring and ultrasonic treatment, thus helping to increase the tensile strength and enhance the antimicrobial activity of the sodium alginate film. The strength and antibacterial tests indicated that the tensile strength of the sodium alginate film increased 225%, and the sodium alginate film also exhibited certain effects on the growth of both *S. aureus* and *E. coli* when 10 wt % MFC/C−BC biocomposite was added. Therefore, the novel sodium alginate composite film can be regarded as a promising material for food packaging.

AUTHOR INFORMATION

Corresponding Author

*Tel: +86 0591-83715175. Fax: +86 0591-83715175. E-mail: fafuhll@163.com.

Funding

The authors acknowledge the Natural Science Foundation of Fujian Province (2012J01064), the Research Fund for Distinguished Young Talents of Fujian Agriculture and Forestry University (XJQ201213), and the Scientific Research Fund of Fujian Agriculture and Forestry University (6210C0313) for financial support.

Notes

The authors declare no competing financial interest.

REFERENCES

(1) Sonkaew, P.; Sane, A.; Suppakul, P. Antioxidant activities of curcumin and ascorbyl dipalmitate nanoparticles and their activities after incorporation into cellulose-based packaging films. *J. Agric. Food Chem.* **2012**, *60*, 5388−5399.

(2) Farris, S.; Introzzi, L.; Fuentes-Alventosa, J. M.; Santo, N.; Rocca, R.; Piergiovanni, L. Self-Assembled pullulan−silica oxygen barrier hybrid coatings for food packaging applications. *J. Agric. Food Chem.* **2012**, *60*, 782−790.

(3) Martínez-Abad, A.; Lagaron, J. M.; Ocio, M. J. Development and characterization of silver-based antimicrobial ethylene−vinyl alcohol copolymer (EVOH) films for food-packaging applications. *J. Agric. Food Chem.* **2012**, *60*, 5350−5359.

(4) Kaushik, A.; Singh, M.; Verma, G. Green nanocomposites based on thermoplastic starch and steam exploded cellulose nanofibrils from wheat straw. *Carbohydr. Polym.* **2010**, *82*, 337−345.

(5) Svagan, A. J.; Hedenqvist, M. S.; Berglund, L. Reduced water vapour sorption in cellulose nanocomposites with starch matrix. *Compos. Sci. Technol.* **2009**, *69*, 500−506.

(6) The, D. P.; Debeaufort, F.; Voilley, A.; Luu, D. Biopolymer interactions affect the functional properties of edible films based on agar, cassava starch and arabinoxylan blends. *J. Food Eng.* **2009**, *90*, 548−558.

(7) Phan, T. D.; Debeaufort, F.; Luu, D.; Voilley, A. Functional properties of edible agar-based and starch-based films for food quality preservation. *J. Agric. Food Chem.* **2005**, *53*, 973−981.

(8) Liu, Y. X.; Peng, J. H.; Sun, B.; Wang, Z. L.; Chen, K. L.; Huang, Y. H. Development and characterization of hemicelluloses edible films. *The 4th International Conference on Pulping, Papermaking and Biotechnology*; 2012; pp 221−224

(9) Xiao, Q.; Tong, Q. Y.; Limc, L. T. Pullulan−sodium alginate based edible films: Rheological properties of film forming solutions. *Carbohydr. Polym.* **2012**, *87*, 1689−1695.

(10) Hambleton, A.; Voilley, A.; Debeaufort, F. Transport parameters for aroma compounds through i-carrageenan and sodium alginate-based edible films. *Food Hydrocolloids* **2011**, *25*, 1128−1133.
(11) Fabra, M. J.; Talens, P.; Chiralt, A. Effect of alginate and λ-carrageenan on tensile properties and water vapour permeability of sodium caseinate−lipid based films. *Carbohydr. Polym.* **2008**, *74*, 419−426.
(12) Fayaz, A. M.; Balaji, K.; Girilal, M.; Kalaichelvan, P. T.; Venkatesan, R. Mycobased synthesis of silver nanoparticles and their incorporation into sodium alginate films for vegetable and fruit preservation. *J. Agric. Food Chem.* **2009**, *57*, 6246−6252.
(13) Wang, L. Z.; Auty, M. A. E.; Kerry, J. P. Physical assessment of composite biodegradable films manufactured using whey protein isolate, gelatin and sodium alginate. *J. Food Eng.* **2010**, *96*, 199−207.
(14) Nakagaito, A. N.; Yano, H. Novel high-strength biocomposites based on microfibrillated cellulose having nano-order-unit web-like network structure. *Appl. Phys. A: Mater. Sci. Process.* **2005**, *80*, 155−159.
(15) Nakagaito, A. N.; Yano, H. The effect of morphological changes from pulp fiber towards nano-scale fibrillated cellulose on the strength properties of high-strength plant fiber based composites. *Appl. Phys. A: Mater. Sci. Process.* **2004**, *78*, 547−552.
(16) Nakagaito, A. N.; Fujimura, A.; Sakai, T.; Hama, Y.; Yano, H. Production of microfibrillated cellulose (MFC)-reinforced polylactic acid (PLA) nanocomposites from sheets obtained by a papermaking-like process. *Compos. Sci. Technol.* **2009**, *69*, 1293−1297.
(17) Lavoine, N.; Desloges, I.; Dufresne, A.; Bras, J. Microfibrillated cellulose−Its barrier properties and applications in cellulosic materials: A review. *Carbohydr. Polym.* **2012**, *90*, 735−764.
(18) Belalia, R.; Grelier, S.; Benaissa, M.; Coma, V. New bioactive biomaterials based on quaternized chitosan. *J. Agric. Food Chem.* **2008**, *56*, 1582−1588.
(19) Jeon, Y. J.; Jkamil, A. Y. V. A.; Shahidi, F. Chitosan as an edible invisible film for quality preservation of herring and Atlantic cod. *J. Agric. Food Chem.* **2002**, *50*, 5167−5178.
(20) Fernandez-saiz, P.; Lagaron, J. M.; Ocio, M. J. Optimization of the film-forming and storage conditions of chitosan as an antimicrobial agent. *J. Agric. Food Chem.* **2009**, *57*, 3298−3307.
(21) Liu, K.; Zhao, G. L.; He, B. H.; Chen, L. H.; Huang, L. L. Immobilization of pectinase and lipase on macroporous resin coated with chitosan for treatment of whitewater from papermaking. *Bioresour. Technol.* **2012**, *123*, 616−619.
(22) Liu, K.; Li, X. F.; Li, X. M.; He, B. H.; Zhao, G.L. Lowering the cationic demand caused by PGA in papermaking by solute adsorption and immobilized pectinase on chitosan beads. *Carbohydr. Polym.* **2010**, *82*, 648−652.
(23) Liu, K.; Zhao, G. L.; He, B. H.; Chen, L. H.; Huang, L. L. Immobilization of lipase on chitosan beads for removal of pitch particles from whitewater during papermaking. *Bioresources* **2012**, *7* (4), 5460−5468.
(24) Aktas, Y.; Andrieux, K.; Alonso, M. J.; Calvo, P.; Gursoy, R. N.; Couvreur, P.; Capan, Y. Preparation and in vitro evaluation of chitosan nanoparticles containing a caspase inhibitor. *Int. J. Pharm.* **2005**, *298*, 378−383.
(25) Bhattarai, N.; Ramay, H. R.; Gunn, J.; Matsen, F. A.; Zhang, M. Q. PEG-grafted chitosan as an injectable thermosensitive hydrogel for sustained protein release. *J. Controlled Release* **2005**, *103*, 609−624.
(26) Mao, H. Q.; Roy, K.; Troung-Le, V. L.; Janes, K. A.; Lin, K. Y.; Wang, Y.; August, J. T.; Leong, K. W. Chitosan−DNA nanoparticles as gene carriers: Synthesis, characterization and transfection efficiency. *J. Controlled Release* **2001**, *70*, 399−421.
(27) Papadimitriou, S. A.; Achilias, D. S.; Bikiaris, D. N. Chitosan-g-PEG nanoparticles ionically crosslinked with poly(glutamic acid) and tripolyphosphate as protein delivery systems. *Int. J. Pharm.* **2012**, *430*, 318−327.
(28) Hou, Q. X.; Liu, W.; Liu, Z. H.; Duan, B.; Bai, L. L. Characteristics of antimicrobial fibers prepared with wood periodate oxycellulose. *Carbohydr. Polym.* **2008**, *74*, 235−240.
(29) Mesquita, J. P.; Donnici, C. L.; Pereira, F. V. Biobased nanocomposites from layer-by-layer assembly of cellulose nanowhiskers with chitosan. *Biomacromolecules* **2010**, *11*, 473−480.
(30) Cheng, Q. Z.; Wang, S. Q.; Rials, T. G. Poly(vinyl alcohol) nanocomposites reinforced with cellulose fibrils isolated by high intensity ultrasonication. *Composites: Part A* **2009**, *40*, 218−224.
(31) Sun, S. L.; An, Q. Z.; Li, X.; Qian, L. Y.; He, B. H.; Xiao, H. N. Synergistic effects of chitosan−guanidine complexes on enhancing antimicrobial activity and wet-strength of paper. *Bioresour. Technol.* **2010**, *101*, 5693−5700.
(32) Iwatake, A.; Nogi, M.; Yano, H. Cellulose nanofiber-reinforced polylactic acid. *Compos. Sci. Technol.* **2008**, *68*, 2103−2106.
(33) Samir, M.; Alloin, F.; Paillet, M.; Dufresne, A. Tangling effect in fibrillated cellulose reinforced nanocomposites. *Macromolecules* **2004**, *37* (11), 4313−4316.
(34) Das, D.; Ara, T.; Dutta, S.; Mukherjee, A. New water resistant biomaterial biocide film based on guar gum. *Bioresour. Technol.* **2011**, *102*, 5878−5883.
(35) Shukla, M. K.; Singh, R. P.; Reddy, C. R. K.; Jha, B. Synthesis and characterization of agar-based silver nanoparticles and nanocomposite film with antibacterial applications. *Bioresour. Technol.* **2012**, *107*, 295−300.
(36) Liu, H.; Du, Y. M.; Wang, X. H.; Sun, L. P. Chitosan kills bacteria through cell membrane damage. *Int. J. Food Microbiol.* **2004**, *95*, 147−155.
(37) Thorsteinsson, T.; Loftsson, T.; Masson, M. Soft antibacterial agents. *Curr. Med. Chem.* **2003**, *10* (13), 1129−1136.
(38) Zhou, N. L.; Meng, N.; Ma, Y. C.; Liao, X. G.; Zhang, J.; Li, L.; Shen, J. Evaluation of antithrombogenic and antibacterial activities of a graphite oxide/heparin−benzalkonium chloride composite. *Carbon* **2009**, *47*, 1343−1350.